PHYSICAL REVIEW B **84**, 041411(R) (2011)

Electronic structure of the delafossite-type CuMO_2 (M = Sc, Cr, Mn, Fe, and Co): Optical absorption measurements and first-principles calculations

Hiroki Hiraga,[1] Takayuki Makino,[2,*] Tomoteru Fukumura,[3,4] Hongming Weng,[5,6] and Masashi Kawasaki[1,2,7,8]

[1]*WPI Advanced Institute for Materials Research, Tohoku University, Sendai 980-8577, Japan*

[2]*Correlated Electron Research Group (CERG), RIKEN Advanced Science Institute (ASI), Wako 351-0198, Japan*

[3]*Department of Chemistry, University of Tokyo, Tokyo 113-0033, Japan*

[4]*PRESTO, Japan Science and Technology Agency, Saitama 332-0012, Japan*

[5]*Research Center for Integrated Science, Japan Advanced Institute of Science and Technology, Ishikawa 923-1292, Japan*

[6]*Institute of Physics, Chinese Academy of Sciences, Beijing 100190, China*

[7]*Quantum Phase Electronics Center and Department of Applied Physics, University of Tokyo, Tokyo 113-8656, Japan*

[8]*CREST, Japan Science and Technology Agency, Tokyo 102-0075, Japan*

(Received 3 April 2011; revised manuscript received 5 June 2011; published 29 July 2011)

We compared the results of first-principles calculations with measured absorption spectra in thin films of delafossite-type CuMO_2 (M = Sc, Cr, Mn, Fe, and Co) taken at 10 K. Two optical transitions were found: one is associated with Cu3d + O2p → Cu3d_{z^2} + 4s observed in all of the CuMO_2 films, and the other is associated with Cu3d + O2p → M3d detected for M = Mn, Fe, and Co. The energy of the former transition showed an unexpected dependence on the atomic number of M. An abrupt change of this energy occurs for M = Cr, which is explained as a result of the interaction between the Cu3d_{z^2} + 4s and M3d bands.

DOI: 10.1103/PhysRevB.84.041411 PACS number(s): 68.55.−a, 71.35.−y, 78.20.−e, 72.80.Ga

The delafossite cuprous compound CuMO_2 is known to exhibit intriguing properties depending on trivalent metal elements M, such as excitonic effects[1] in $CuScO_2$, p-type conductivity[2] in $CuAlO_2$, and multiferroicity with ferroelectricity and ferromagnetism[3,4] in $CuCrO_2$ and $CuFeO_2$. Their electronic structures have to be systematically studied for a deeper understanding of their properties.

We used this to examine the influence of 3d orbital occupancy of transition metals (TM) on properties in CuMO_2. The optical transitions (E_g^B) appear in the visible region due to charge-transfer (CT) excitations to the TM 3d orbitals, as observed in LaMO_3,[5] Sr_2MO_4,[6] and CuMO_2.[7–9] In LaMO_3, the TM-related gap energy decreased with an increase in atomic numbers from Cr to Ni, the dependence of which has been explained in terms of atomic ionization energies and of Madelung potentials.[5] There is an optical gap (E_g^A) in the higher energy region for CuMO_2, attributed to *dipole-allowed* Cu3d + O2p → Cu3d_{z^2} + 4s transition.[1] This is in contrast to Cu_2O,[10] which is *dipole forbidden*. The layered structure can be viewed as a natural superlattice composed of Cu_2O dumbbells and the wider band-gap insulator M_2O_3 as shown in the inset of Fig. 1 (M = Sc). In the naturally low-dimensional structure, hybridization of Cu and O orbitals[2,11] results in a direct gap[1] accompanied by an excitonic effect.[1]

In this work, the interaction between excitons and d-orbital ions was studied for CuMO_2 (M = Sc, Cr, Mn, Fe, and Co) at 10 K by absorption spectroscopy. Such an interaction was investigated in diluted magnetic semiconductors[12,13] such as $Cd_{1-x}M_xTe$ (M = Cr, Mn, Fe, and Co), with magnetic polaron effects. There has been no study on the effect of *quasi-low-dimensional* excitons. An anomalous M-element dependence of the E_g^A energy was found, and this dependence was explained by first-principles calculations in terms of the relative positions of M3d and Cu3d_{z^2} + 4s bands.

CuMO_2 thin films were grown on $MgAl_2O_4$ (111) substrates (cubic structure with a = 8.083 Å) and sapphire (0001) substrates (hexagonal structure with a = 4.759 Å and c = 12.993 Å) using a pulsed laser deposition.[14] Highly crystalline films were obtained on $MgAl_2O_4$ substrates for M = Sc and Mn,[1,7] whereas sapphire gave rise to better crystallinity in M = Cr, Fe, and Co. These substrates were prepared to be atomically flat by annealing in a furnace. A hot-press method was used to prepare targets for M = Mn and Fe (M = Sc, Cr, and Co). To determine the crystallographic data, powder x-ray diffraction (XRD) and high-resolution four-circle XRD were used for 150-nm-thick films. Optical absorption spectra were measured at 10 K.

Figure 1 shows reciprocal space maps of XRD around $(10\bar{1}\underline{1}\underline{4})$ of CuMO_2 (M = Cr, Fe, and Co) having a trigonal structure and sapphire $(20\bar{2}10)$ asymmetric diffractions. Mismatches of the hexagonal unit cell parameters between bulk and thin films were as small as 1.2%,[15,16] indicating that the film lattices are relaxed. The x-ray pole figures for the $(10\bar{1}8)$ diffraction peak of CuMO_2 and $(10\bar{1}2)$ of the sapphire substrate revealed two domains with in-plane 60° rotation. This is consistent with the previously observed features for a $CuGaO_2$ on sapphire.[17] The films have single phases without other impurity phases. Crystallographic data of CuMO_2 films (M = Sc and Mn) are found elsewhere.[1,7] The inset shows a typical crystal structure and epitaxial relationship of the film to the substrate. Perpendicular to the plane, the octahedral is connected by a Cu-O-Cu dumbbell structure.[1]

The absorption spectra were analyzed by first-principles calculations in which the accurate all-electron full-potential literalized augmented plane-wave method implemented in WIEN2k package was used.[15] To describe the 3d electrons correctly, on-site Coulomb interaction is treated by a generalized gradient approximation +U (GGA+U) method. Despite its chemical trend, we used a value of U independent of M *for simplicity*. The use of U = 4.0 eV gave results compared reasonably well with experimental data. The experimental geometrical structure was used for calculation. Despite its

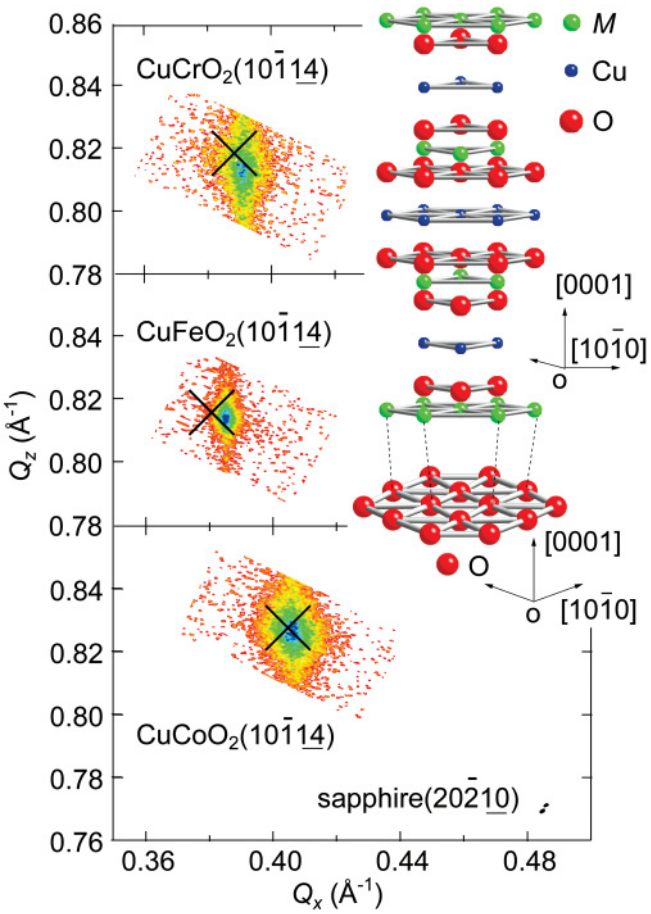

FIG. 1. (Color online) Reciprocal space contour map around CuMO_2 (10$\bar{1}$14) and sapphire (20$\bar{2}$10) diffractions. Crosses denote the corresponding peak positions for the bulk compounds. Inset shows the epitaxial relationship and definitions of the respective indices.

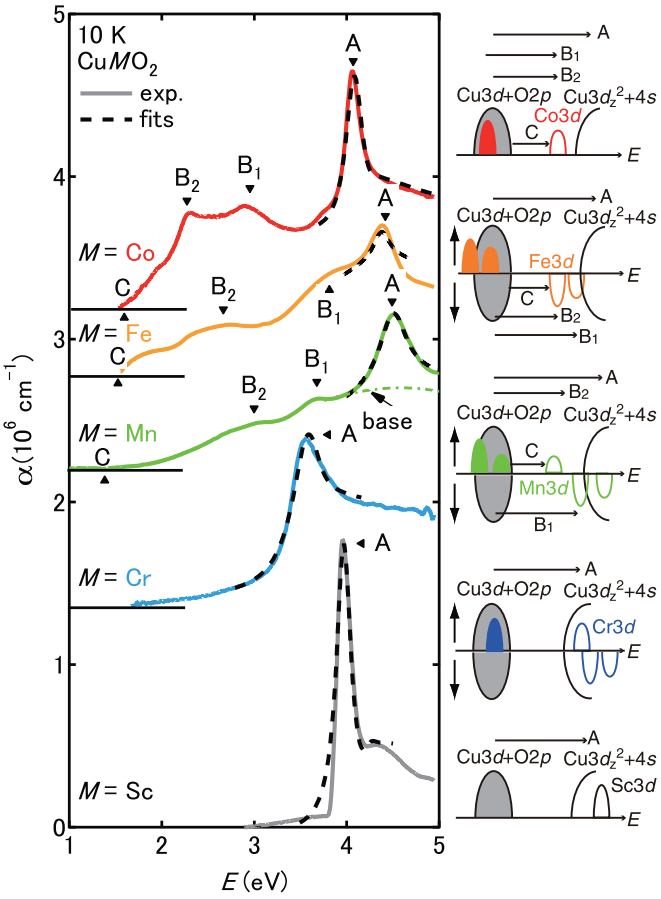

FIG. 2. (Color online) Absorption spectra (solid lines) of CuMO_2 (M = Sc, Cr, Mn, Fe, and Co) thin films measured at 10 K. Dashed lines represent fits to the experimental data based on a modified Elliott model, with a baseline (a dash-dotted line). Schematic energy diagrams, concluded from first-principles calculations, are shown in the right panel. Arrows indicate transitions corresponding to the observed absorption peaks.

noncollinear magnetic ordering of $CuCrO_2$, we take, the antiferromagnetic ordering[19] as measured in $CuFeO_2$. For $CuMnO_2$, the experimental antiferromagnetic ordering[7] is used for calculation.

Experimental absorption spectra are shown by solid lines in Fig. 2 for CuMO_2 films. The absorption is negligible below a sharp peak "A" in $CuScO_2$ and $CuCrO_2$, while there are discernible peaks "B_1" and "B_2" and an absorption tail "C" for the other compounds (M = Mn, Fe and Co). A better understanding of the difference in characters of peaks requires insights into their electronic structures. We drew a schematic energy-level diagram from our first-principles calculations as shown in the right panel of Fig. 2. Starting from the lowermost trace for M = Sc and Cr, the transition Cu3d + O2p $\rightarrow$ unoccupied M3d states has a larger energy than that of the Cu3d + O2p $\rightarrow$ Cu3d_{z^2} + 4s gap. The latter transition can be found as a common absorption peak of "A," related to the excitation in Cu-O-Cu structures. Such a low-dimensional structure leads to the van Hove singularity in density of states for both valence and conduction bands, as shown by "Cu3d" in Fig. 3(a). This can account partially for the narrow width of this peak. Here, not only the Cu4s but also the Cu3d_{z^2} orbitals contribute to the conduction band minima (CBM) due to the hybridization effect. This is because the actual charge state of Cu ions is slightly larger than +1, being the formal charge state of CuMO_2. The absorption peak "A" is assigned to exciton states with the quantum number of n = 1, followed by higher-lying continuum absorption,[20] we evaluate their binding energies. Because of ambiguity in determining the energy of the continuum, we analyzed the line shape based on a modified Elliott model[1] by relying on the exciton energy, the absorption coefficients at the n = 1 state, and at the continuum.[21] The results of fitting are shown by dashed lines in Fig. 2 with a baseline determined by contributions from other peaks. The excitonic binding energies are 380, 330, 520, 450, and 320 meV for M = Sc, Cr, Mn, Fe, and Co, respectively. All the values are larger than that of Cu_2O (150 meV)[10] and approximately proportional to the energy E_g^A. we define the *absorption peak energy* as E_g^A.

The peaks B_1 and B_2 are assigned to the M-related transition of Cu3d + O2p $\rightarrow$ M3d or d-d transition of M3d. They are similar to the CT excitation from O2p to M3d upper Hubbard states with its ligand field splitting in the 3d orbital as observed in LaMO_3.[5] The excitons do not seem to affect on

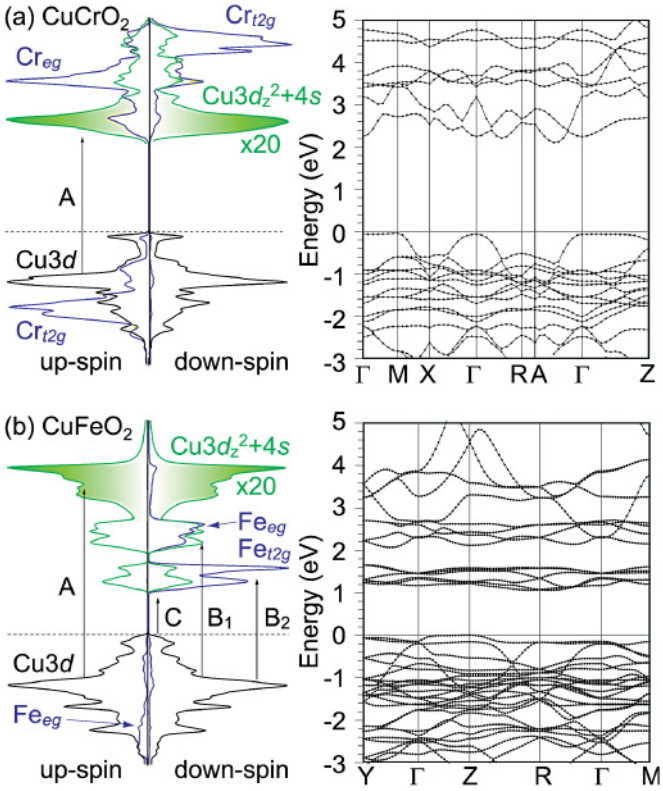

FIG. 3. (Color online) Density of states (left panel) and band structure (right panel) of $CuCrO_2$ (a) and $CuFeO_2$ (b) deduced from GGA+U (U = 4.0 eV) calculations. Arrows indicates interband transitions corresponding to the absorption peaks shown in Fig. 2. Note that the density of states for Cu3d_z^2 + 4s is magnified for clarification.

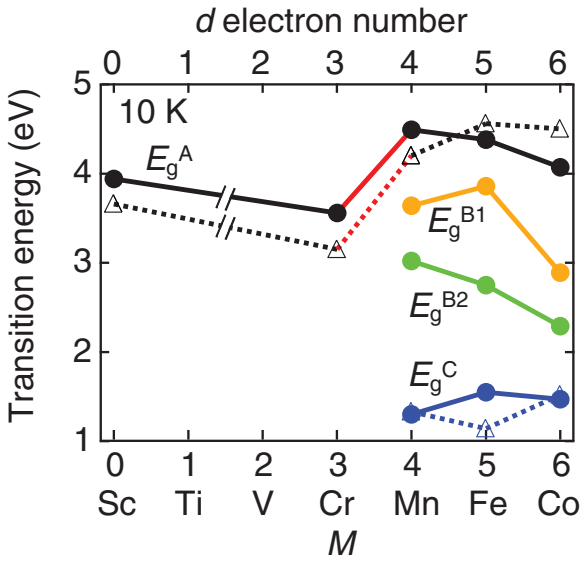

FIG. 4. (Color online) Transition energies, E_g^A, E_g^{B1}, E_g^{B2}, and E_g^C, of absorption spectra shown in Fig. 2 are plotted against the number of 3d electrons in M^{3+} ions of CuMO_2 (M = Sc, Cr, Mn, Fe, and Co) thin films. Closed circles indicate experimental values, and open triangles refer to the first-principles calculation results. An abrupt change occurs in E_g^A between $CuCrO_2$ and $CuMnO_2$.

the line shapes because they are close to that of first-principles calculations. The energies of tails C correspond to those of the lowest band gaps (E_g^C).

The electronic structure of $CuCrO_2$ is straightforward as shown in Fig. 3(a). The film has absorption at $E_g^A = 3.56$ eV, because the occupied t_{2g} and the empty e_g levels of Cr^{3+} are energetically far away from the valence band maximum (VBM) and the CBM, respectively. Unlike previous studies,[22,23] other lower-lying transitions were not observed in our films, due to the single-phase nature and high orientation of the films.

In $CuMnO_2$, the lowest unoccupied band is mainly the Mn $d_{x^2-y^2}$ orbital because of Jahn-Teller splitting of the e_g band in Mn^{3+}, where three electrons are in spin majority t_{2g} bands, and one is in the spin majority d_{z^2} orbital. The Cu3d_z^2 + 4s orbitals are higher than the Mn $d_{x^2-y^2}$ orbitals and mixed with the *spin minority* Mn t_{2g} states. The *spin minority* Mn e_g states are in a higher level. The two lower-lying peaks B_2 at 3.0 eV and B_1 at 3.7 eV are assigned to CT excitations to the above-mentioned final states, i.e., Cu3d + O2p → Mn $d_{x^2-y^2}$ (E_g^{B2}) and Cu3d + O2p → Mn t_{2g} (E_g^{B1}), respectively.

In $CuFeO_2$, four absorption peaks were identified at 4.38 (A), 3.85 (B_1), 2.80 (B_2), and 1.55 (C) eV. According to the calculated band structure shown in Fig. 3(b), B_1 and B_2 are assigned to the transitions of Cu3d + O2p → Fe e_g and of Cu3d + O2p → Fe t_{2g}. These peak energies are higher than those reported in the literature.[9,24] The previous values have been determined from photo-electrochemical spectra. The interpretation of such a spectrum is complex, leading to an inaccurate estimate.

TM-related absorption peaks were also observed in $CuCoO_2$. Our band structure calculations indicated that the Co^{3+} ions are in a nonmagnetic state with fully occupied t_{2g} orbitals and empty e_g orbitals, which is consistent with a previous report on magnetic properties.[24] The fully occupied t_{2g} orbitals are located about 1.0–2.0 eV below the highest occupied Cu3d + O2p orbitals, i.e., VBM. The empty e_g orbitals are located ∼2.0 eV higher than the VBM and ∼1.5 eV lower than the CBM. Therefore, the B_2 peak is assigned to transition of Cu3d + O2p → Coe_g. The assignment of B_1 is associated with the Co d-d transition inside Co3d (t_{2g}→e_g) ions. The d-d optical transition may be partially dipole allowed due to a lower symmetry of the delafossite structure.[26]

Figure 4 shows experimental values of the energies E_g^A, E_g^{B1}, E_g^{B2}, and E_g^C along with the theoretical E_g^A and E_g^C. The energies E_g^{B1} and E_g^{B2} decrease monotonically from M = Mn to Co. This chemical trend is consistent with that in LaMO_3, explained in terms of chemical trends of the atomic ionization energies and of Madelung potentials.[5] There is an abrupt jump in E_g^A (a red line in Fig. 4) at M = Cr despite the same origin for the relevant transition.

The reason for the jump in E_g^A is understood from the electronic structure diagram shown in Fig. 2. The position of the Cu3d_{z^2} + 4s orbital is influenced by the unoccupied M3d orbitals having an apparent chemical trend, which results in the above-mentioned M-dependence of E_g^A. Let us discuss the electronic structures of CuMO_2 around the jump, i.e., $CuCrO_2$

and $CuFeO_2$. $CuMnO_2$ was not adopted for this comparison because of the different crystal system (monoclinic).[7,27] As shown in Fig. 3(a), the unoccupied *d* orbital of Cr3*d* lies higher in energy than Cu3d_{z^2} + 4*s* bands, resulting in Cu3d_{z^2} + 4*s* bands being pushed downward. The unoccupied *d* orbitals are located lower than Cu3d_{z^2} + 4*s* bands later 3*d* elements such as Mn, Fe, and Co, resulting in the latter band being pushed higher. Repulsive interaction between the two bands determines the position of the CBM, while the VBM remains unchanged. The energy of E_g^A in $CuCrO_2$ is significantly smaller than that in $CuFeO_2$, as shown by arrows with "A" in the left panels of Fig. 3. The theoretical calculations support this interpretation; the E_g^A are in agreement with experiments as shown in Fig. 4.

The optical properties of CuMO_2 are characterized by strong interaction between 3*d* electrons and excitons. These materials can thus be regarded as a suitable system to investigate the excitonic effect on photo-induced spin dynamics. It should be noted that the importance of Coulomb interaction for photo-dynamics has been recently pointed out even in ferromagnetic metals.[28]

In summary, we measured absorption spectra in CuMO_2 (M = Sc, Cr, Mn, Fe, and Co) at 10 K. Absorption peaks corresponding to the excitonic transition between Cu3*d* + O2*p* and Cu3d_{z^2} + 4*s* bands were commonly observed. CT and *d*-*d* transitions involving 3*d* orbitals of M were identified. The results of first-principles calculations systematically explain the energy positions of the above-mentioned transitions as a function of M taking into account the relative positions between Cu3d_z^2 + 4*s* and M3*d* bands.

We would like to thank T. Arima and I. Hamada for discussions. This research was, in part, supported by Nano-Materials Functionality Creation Research Project for Young Scientists in IMR (T.F.), KAKENHI (21104502) from MEXT, Japan (T.M.) and Funding Program for World-Leading Innovative R&D on Science and Technology (FIRST) of JSPS. H. W. acknowledges the support from IOP, CAS (Y0K5015T31) and computing facilities in JAIST.

*tmakino@riken.jp

[1] H. Hiraga, T. Makino, T. Fukumura, A. Ohtomo, and M. Kawasaki, Appl. Phys. Lett. **95**, 211908 (2009)

[2] H. Kawazoe, M. Yasukawa, H. Hyodo, M. Kurita, H. Yanagi, and H. Hosono, Nature **389**, 939 (1997).

[3] T. Kimura, J. C. Lashley, and A. P. Ramirez, Phys. Rev. B **73**, 220401 (2006).

[4] S. Seki, Y. Onose, and Y. Tokura, Phys. Rev. Lett. **101**, 067204 (2008).

[5] T. Arima and Y. Tokura, J. Phys. Soc. Jpn. **64**, 2488 (1995).

[6] J. Matsuno, Y. Okimoto, M. Kawasaki, and Y. Tokura, Phys. Rev. Lett. **95**, 176404 (2005).

[7] H. Hiraga, T. Fukumura, T. Makino, A. Ohtomo, A. Ohkubo, H. Kimura, and M. Kawasaki, Appl. Phys. Lett. **95**, 032109 (2009).

[8] F. A. Benko and F. P. Koffyberg, J. Phys. Chem. Solids **48**, 431 (1987).

[9] F. A. Benko and F. P. Koffyberg, Mater. Res. Bull. **21**, 753 (1986).

[10] V. T. Agekyan, Phys. Status Solidi A **43**, 11 (1977).

[11] H. Kawazoe, H. Yanagi, K. Ueda, and H. Hosono, MRS Bull. **25**, 28 (2000).

[12] M. Herbich, A. Twardowski, D. Scalbert, and A. Petrou, Phys. Rev. B **58**, 7024 (1998).

[13] U. Gennser, X. C. Liu, T. Q. Vu, D. Heiman, T. Fries, Y. Shapira, M. Demianiuk, and A. Twardowski, Phys. Rev. B **51**, 9606 (1995).

[14] The growth temperatures were 650, 700, 500, 700 and 500 °C for M = Sc, Cr, Mn, Fe, and Co, respectively. The oxygen pressures were 1×10^{-3}, 1×10^{-3}, 1×10^{-4}, 1×10^{-4}, and 1×10^{-3} Torr. The laser repetition was 5 Hz, and the deposition rate was $\approx 2\times 10^{-3}$ nm/pulse.

[15] M. A. Marquardt, N. A. Ashmore, and D. P. Cann, Thin Solid Films **496**, 146 (2006).

[16] The hexagonal unit cell parameters for a bulk (a film) were a = 2.975, 3.035, and 2.849 Å (a = 2.95, 3.00, and 2.84 Å). The constants of c lattices were c = 17.096, 17.166, and 16.920 Å (c = 17.180, 17.140, and 16.930 Å).

[17] K. Ueda, T. Hase, H. Yanagi, H. Kawazoe, H. Hosono, H. Ohta, M. Orita, and M. Hirano, J. Appl. Phys. **89**, 1790 (2001).

[18] P. Blaha, K. Schwarz, G. K. H. Madsen, D. Kvasnicka, and J. Luitz, *WIEN2k, An Augmented Plane Wave + Local Orbitals Program for Calculating Crystal Properties* (Karlheinz Schwarz, Techn. Universität, Wien, Austria, 2001), ISBN 3-9501031-1-2.

[19] V. Eyert, R. Frésard, and A. Maignan, Phys. Rev. B **78**, 052402 (2008).

[20] Individual lines of $n > 1$ excitons could not be resolved because of broadening due to impurity scatterings.

[21] S. Gilliland, J. F. Sánchez-Royo, J. Pellicer-Porres, A. Segura, A. Muñoz, P. Rodríguez-Hernández, and J. López-Solano, Thin Solid Films **516**, 1431 (2008).

[22] D. Li, X. Fang, Z. Deng, S. Zhou, R. Tao, W. Dong, T. Wang, Y. Zhao, G. Meng, and X. Zhu, J. Phys. D **40**, 4910 (2007).

[23] S. Mahapatra and S. A. Shivashankar, Chem. Vap. Deposition **9**, 238 (2003).

[24] K. P. Ong, K. Bai, P. Blaha, and P. Wu, Chem. Mater. **19**, 634 (2007).

[25] M. Beekman, J. Salvador, X. Shi, G. S. Nolas, and J. Yang, J. Alloys Compd. **489**, 336 (2010).

[26] S. Sugano, Y. Tanabe, and H. Kamimura, *Multiplets of Transition-Metal Ions in Crystals* (Academic, New York, 1970).

[27] M. Trari, J. Topfer, P. Dordor, J. C. Grenier, M. Pouchard, and J. P. Doumerc, J. Solid State Chem. **178**, 2751 (2005).

[28] M. Krauss, T. Roth, S. Alebrand, D. Steil, M. Cinchetti, M. Aeschlimann, and H. C. Schneider, Phys. Rev. B **80**, 180407(R) (2009).